

promoting access to White Rose research papers



Universities of Leeds, Sheffield and York
<http://eprints.whiterose.ac.uk/>

This is an author produced version of an article published in **Applied Physics Letters**.

White Rose Research Online URL for this paper:

<http://eprints.whiterose.ac.uk/76109/>

Published article:

Valavanis, A, Dean, P, Scheuring, AHW, Salih, M, Stockhausen, A, Wuensch, S, Il'in, KS, Chowdhury, S, Khanna, SP, Siegel, M, Davies, AG and Linfield, EH (2013) *Time-resolved measurement of pulse-to-pulse heating effects in a terahertz quantum cascade laser using an NbN superconducting detector*. Applied Physics Letters, 103 (6). 061120-1 - 061120-4 (4).

<http://dx.doi.org/10.1063/1.4818584>

Time-resolved measurement of pulse-to-pulse heating effects in a terahertz quantum cascade laser using an NbN superconducting detector

A. Valavanis,^{1, a)} P. Dean,¹ A. Scheuring,² M. Salih,¹ A. Stockhausen,² S. Wuensch,² K. Il'in,² S. Chowdhury,¹ S. P. Khanna,¹ M. Siegel,² A. G. Davies,¹ and E. H. Linfield¹

¹⁾*Institute of Microwaves and Photonics, School of Electronic and Electrical Engineering, University of Leeds, Leeds LS2 9JT, United Kingdom*

²⁾*Institute of Micro- and Nanoelectronic Systems, Karlsruhe Institute of Technology (KIT), 76187, Karlsruhe, Germany*

(Dated: 30 July 2013)

Joule heating causes significant degradation in the power emitted from terahertz-frequency quantum-cascade lasers (THz QCLs). However, to date, it has not been possible to characterize the thermal equilibration time of these devices, since THz power degradation over sub-millisecond time-scales cannot be resolved using conventional bolometric or pyroelectric detectors. In this letter, we use a superconducting antenna-coupled niobium nitride detector to measure the emission from a THz QCL with a nanosecond-scale time-resolution. The emitted THz power is shown to decay more rapidly at higher heat-sink temperatures, and in steady-state the power reduces as the repetition rate of the driving pulses increases. The pulse-to-pulse variation in active-region temperature is inferred by comparing the THz signals with those obtained from low duty-cycle measurements. A thermal resistance of 8.2 ± 0.6 K/W is determined, which is in good agreement with earlier measurements, and we calculate a 370 ± 90 - μ s bulk heat-storage time, which corresponds to the simulated heat capacity of the device substrate.

PACS numbers: 42.55.Px, 66.70.Df, 85.25.Pb

Keywords: terahertz quantum cascade lasers, thermal characterisation, superconducting terahertz-radiation detectors

Terahertz-frequency quantum-cascade lasers (THz QCLs) are compact semiconductor sources of high-power, narrowband THz radiation.¹ Although peak THz powers greater than 200 mW (pulsed) can be achieved at low temperatures,² QCL performance degrades as either the heat-sink temperature, or the pulse repetition rate is increased. This is primarily a result of the population inversion in the laser subbands being degraded by thermal backfilling and thermally-activated electron-phonon interactions.³ The effect is exacerbated by the fact that THz QCLs typically require several watts of electrical input power, which leads to significant Joule heating within the active-region (AR) of the device, causing its temperature to be significantly higher than that of the heat-sink. This is particularly the case for QCLs based on resonant-phonon (RP) depopulation, where large operating biases are needed, and parasitic current channels increase the threshold current density significantly.⁴ Such limitations mean that lasing cannot currently be achieved at heat-sink temperatures above 200 K (pulsed)⁵ or 117 K (continuous-wave).⁶

It is clear that to optimize THz QCL performance, it is essential to characterize their heat extraction fully. However, the thermal relaxation path involves several regions with significant variation in heat capacity and thermal conductance, each being characterized by a different thermal time-constant. This results in a complicated time-variation in device temperature when driven by a

pulsed electrical source,^{7,8} and a range of thermal characterization techniques have been used to investigate such thermal effects experimentally. The steady-state thermal resistance has been inferred by measuring the time-averaged THz power using a pyroelectric detector.⁹ Alternatively, time-resolved microprobe photoluminescence (PL) techniques allow sampling of the rapid temperature-variations at specific positions within a QCL, over the duration of a single laser pulse. This allowed thermal time constants on the order of 1 μ s and 10 μ s to be determined within, and slightly below, the AR, respectively.⁸ However, the *total* thermal equilibration time of a QCL (and hence the THz power stabilization time) is determined by bulk heat accumulation within the device. Heat-transfer modeling predicts this to occur over ~ 100 μ s time scales,⁷ which are much longer than those studied in PL measurements, and yet much shorter than the response times of conventional THz detectors (typically milliseconds for cryogenically-cooled semiconductor bolometers).

We present time-resolved measurements of the pulsed THz emission from a THz QCL, using a superconducting niobium nitride (NbN) detector with a response time on the order of 30 ps.^{10,11} This allows continuous high-bandwidth data acquisition rather than discrete sampling (as is the case in PL studies) over the duration of a laser pulse-train. From our ultrafast THz emission measurements, we determine the pulse-to-pulse increase in AR temperature and infer a thermal resistance, which is in good agreement with values obtained using previously-reported techniques. In contrast to earlier works, however, we also extract the bulk heat-storage time-constant,

^{a)}Electronic mail: a.valavanis@leeds.ac.uk

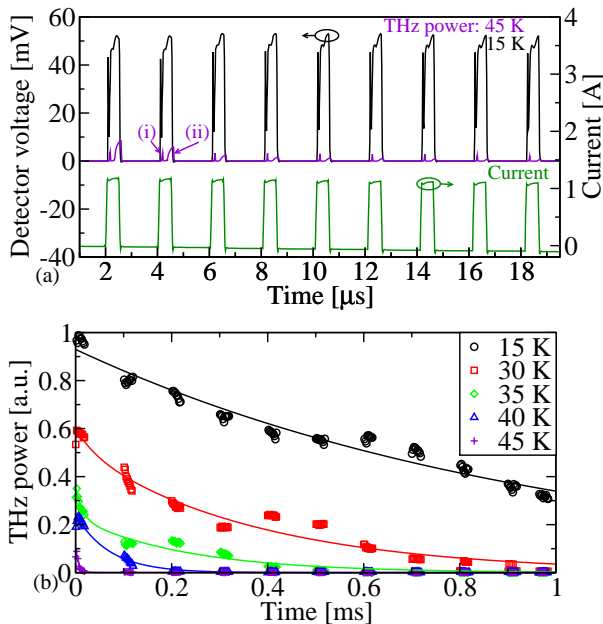


FIG. 1. (a) Driving current and corresponding THz power at heat-sink temperatures of 15 and 45 K. The ‘(i)’ and ‘(ii)’ labels in the 45-K trace indicate the ‘pre-pulse’ and ‘main pulse’ features in the THz emission. (b) Time-averaged power in THz pulses sampled across a 1-ms-long pulse-train for a range of heat-sink temperatures. Solid lines show regressions to bi-exponential decay functions. A 500-kHz pulse-repetition rate was used in all cases.

and show that this corresponds to the heat-capacity of the device substrate.

For our measurements, a 3.1-THz QCL based on an RP depopulation scheme¹² was processed into a semi-insulating surface-plasmon (SISP) ridge waveguide with dimensions $10 \times 140 \times 850 \mu\text{m}^3$. The laser was attached to the cold-finger of a continuous-flow helium cryostat and driven by an Agilent 8114A pulse generator. A pulse-width of 500 ns was used throughout this work and pulse repetition-rates were adjusted through the range 100–500 kHz, giving pulse-separations in the range 9.5–1.5 μs , respectively. Current pulses were measured using an inductive current-probe with a 3.5-ns rise-time. The pulse train was modulated electrically by a 500-Hz square-envelope, allowing a 1-ms-long cooling period between each sequence of driving pulses. The THz radiation emitted by the QCL was collimated and focused onto an NbN detector, within a separate cryostat, as described in Ref. 13. The intrinsic response time of the detector was around 30 ps,^{10,11} and a time-resolution of 1.1 ns was estimated using the method in Ref. 14. The detector response was confirmed to be linear with respect to both the instantaneous incident THz power, and the integrated power (i.e., the energy) over a THz pulse.¹³

Initially, the pulse-repetition rate was fixed at 500 kHz and the heat-sink temperature, T_H , was varied between 15 and 45 K. Fig. 1(a) shows the driving current pulses and the corresponding NbN detector signals at $T_H = 15$ K

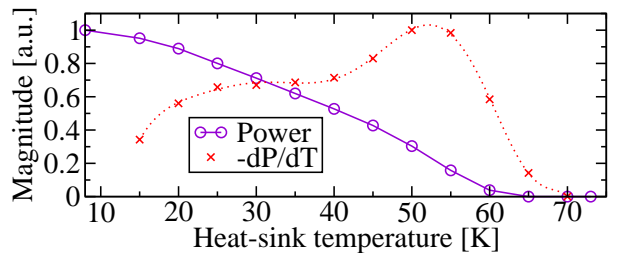


FIG. 2. Normalized THz power emission from the QCL and its derivative with respect to T_H , when driven by a continuous train of 500-ns-long, 12.9-V pulses with a repetition rate of 1 kHz (i.e., 0.05% duty-cycle). Solid lines show polynomial regressions to the data.

and 45 K, acquired over the first 20 μs of the 1-ms-long pulse-train. A baseline shifting algorithm was used to compensate for ac-coupling effects in the detector. Although QCLs do not exhibit relaxation oscillations¹⁵ the intrapulse power responds to driving-current transients, which are principally caused by impedance mismatch.¹³ An initial spike in THz power [label (i) in Fig. 1(a)] is caused by a ripple on the rising-edge of the current pulse briefly exceeding the lasing threshold. A second, longer THz emission (ii) corresponds to the plateau of the current pulse. The current and voltage during the plateau were measured as 1.17 A and 12.9 V, respectively, and were constant from pulse to pulse.

The complex shape of the THz pulses makes it impractical to determine temperature variation within an individual pulse. However, the *pulse-to-pulse* variation may be inferred by examining the time-averaged THz power during successive pulses. At $T_H = 15$ K, the THz emission does not change significantly from pulse-to-pulse. At $T_H = 45$ K, however, pulse-to-pulse heating effects are clearly visible. As expected, the initial pulse amplitude is reduced, owing to the (time-invariant) direct effect of T_H on device performance. Additionally, the energy in successive pulses decays monotonically over time, indicating slow heat accumulation in the bulk of the device.

In order to perform a quantitative analysis of power degradation over the complete 1-ms-long pulse train, 20- μs -long sequences of pulses were sampled at 100- μs intervals and the time-averaged power was calculated for each pulse. As shown in Fig. 1(b), the power decreases over time for all heat-sink temperatures. Indeed, for $T_H \geq 30$ K, the signal decays to the detection noise floor within the period of observation, implying that the maximum operating temperature of the AR had been exceeded as a result of pulse-to-pulse heating.

The increased sensitivity of the THz emission to heat accumulation at higher T_H values may be explained by considering Fig. 2, which shows the relationship between THz power and T_H at low duty-cycle. This measurement was obtained using a helium-cooled Ge bolometer, with the QCL being driven by 500-ns pulses at a 1-kHz repetition rate (0.05% duty-cycle). Although the THz power

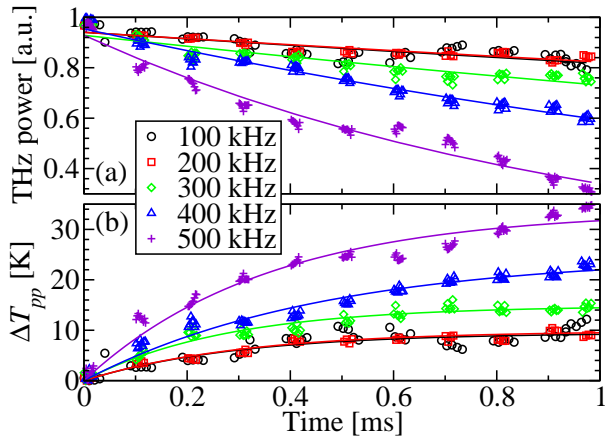


FIG. 3. (a) Time-averaged amplitude of each 500-ns THz pulse sampled across a 1-ms-long pulse-train. Results are shown for $T_H = 15$ K and varying repetition rates. Solid lines show regressions to exponential decay functions. (b) Pulse-to-pulse temperature increase, inferred from THz power measurements. Solid lines show regressions to an equivalent constant heat-flux model (Eqn. 2).

varies in a complex manner within the pulse, the measured time-averaged power can be approximated as the instantaneous power midway through the pulse. Under these low-duty-cycle driving conditions, the active-region temperature T_{AR} can be assumed to settle to T_H between successive pulses. The temperature at the middle of each pulse is, therefore, equal to the sum of T_H and an additional intra-pulse heating term, ΔT_{intra} that represents the rapid heating effect described in Ref. 8.

If the thermal properties of the materials are only weakly dependent on temperature, then ΔT_{intra} represents a constant offset between T_H and T_{AR} . As such, the derivative of the power-temperature relationship, $dP/dT_{AR} = dP/dT_H$, shown in Fig. 2, indicates that small increases in AR temperature cause a much greater degradation in THz power at temperatures around 45 K than at lower AR temperatures, in agreement with the results in Fig. 1(b), and illustrating clearly the importance of bulk heat-storage at high duty-cycles.

Bulk heat-storage is much slower than intra-pulse heating, and so the two effects contribute to the device temperature independently. The instantaneous temperature at the middle of the n^{th} pulse is then given by

$$T_{AR,n} \approx T_H + \Delta T_{intra} + \Delta T_{pp,n}, \quad (1)$$

where $\Delta T_{pp,n}$ is the net pulse-to-pulse temperature rise after n pulses. If pulse-to-pulse heating occurs over time-scales that are significantly larger than the pulse repetition period, then the pulsed heat source may be modeled as an equivalent steady-state (time-averaged) heat flux of γQ , where γ is the duty-cycle of the source and $Q = IV = 1.17 \text{ A} \times 12.9 \text{ V} = 15.1 \text{ W}$ is the electrical driving power during the pulse. A first-order lumped-

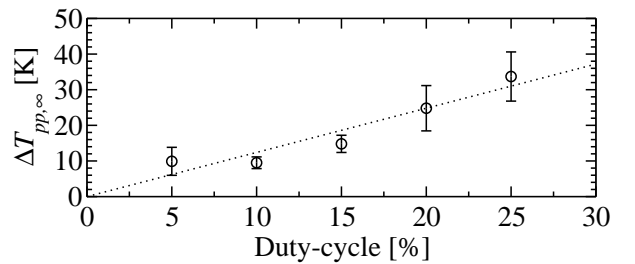


FIG. 4. Final bulk temperature offset as a function of duty cycle, for a QCL driven by a 500-ns pulse train, with 15-K heat-sink temperature. The dotted line shows a linear regression to the data.

component thermal model then yields

$$\Delta T_{pp,n} = R_{th} \gamma Q \left[1 - \exp \left(-\frac{t_n}{R_{th} C_{bulk}} \right) \right], \quad (2)$$

where R_{th} and C_{bulk} are respectively the effective thermal resistance and the bulk heat capacity. The time at the middle of the n^{th} pulse is $t_n = n/f + 0.5t_p$, where f is the repetition rate and $t_p = 500$ ns is the pulse-width.

Under these approximations, ΔT_{intra} is identical in each pulse. The THz power emitted in the n^{th} pulse, therefore, depends only on the heat-sink temperature and bulk heat accumulation, and may be written using the functional form $P_{out}(T_H + \Delta T_{pp,n})$. Additionally, $\Delta T_{pp,n}$ is independent of T_H if R_{th} and C_{bulk} are approximately temperature independent. The pulse-to-pulse temperature rise may, therefore, be inferred by comparing the measured THz power in each pulse with the low duty-cycle reference, $P_{out}(T_H)$, in Fig. 2.

Since some signals in Fig. 1(b) decay below the noise-floor within the observation period, an alternative data set was used for this thermal analysis, in which the repetition rate was varied. A constant $T_H = 15$ K was now used, in order to reduce the THz power decay rate and maintain a measurable signal over 1 ms. Fig. 3(a) shows that the THz power degradation rate increases as the pulse repetition rate was varied from 100 to 500 kHz, as expected for bulk heat accumulation. Furthermore, power degradation is observed even at $f = 100$ kHz indicating that the time constant for pulse-to-pulse heating, $\tau = R_{th} C_{bulk}$, is greater than the 9.5- μ s pulse separation.

In each case, the inferred pulse-to-pulse temperature variation, shown in Fig. 3(b), approaches a final quasi-equilibrium value within the 1-ms observation period. Although PL measurements show a much steeper temperature gradient across the AR than the substrate during continuous-wave operation,¹⁶ theoretical work predicts a more complex situation in pulsed mode.⁷ In this case, the temperature difference between the top and bottom of the AR fluctuates rapidly within each pulse, while the temperature at the bottom of the AR increases gradually over many pulses owing to the large heat capacity of the substrate. Since we use the THz emission as the thermometric property, the *absolute value* of $T_{AR,n}$ would

represent both a temporal average (over the duration of the n^{th} pulse) and a spatial average of the temperature across the active-region (weighted by the photon emission at each point). However, in Fig. 3(b) we only infer the slow *pulse-to-pulse change* in $T_{\text{AR},n}$, rather than its absolute value, and this is principally influenced by heat accumulation in the substrate.

The solid lines in Fig. 3(b) show that regressions to the bulk heating model in Eqn. 2 match the data accurately in all cases. The final (quasi-equilibrium) temperature offset is related analytically to the duty-cycle according to $\Delta T_{pp,\infty} = R_{\text{th}}\gamma Q$, and a linear regression to this form (Fig. 4) yields $R_{\text{th}} = 8.2 \pm 0.6 \text{ K/W}$. This corresponds to a normalized thermal conductance, $G_{\text{th}} = (R_{\text{th}}A)^{-1} = 100 \pm 7 \text{ W K}^{-1}\text{cm}^{-2}$, where A is the waveguide area. This is comparable with previously published values ($G_{\text{th}} = 300$ or $210 \text{ W K}^{-1}\text{cm}^{-2}$, depending on analysis method), from time-averaged power measurements of a device with a double-metal waveguide,⁹ and also with those obtained using PL measurements of an SISF device ($G_{\text{th}} = 41 \text{ W K}^{-1}\text{cm}^{-2}$ in pulsed operation,⁸ and $39 \text{ W K}^{-1}\text{cm}^{-2}$ in continuous operation¹⁷).

TABLE I. Thermal time-constants and corresponding heat capacities of the THz QCL at a range of pulse-repetition rates. Data are obtained from a regression of the inferred T_{AR} values to the form in Eqn. 2.

| f [kHz] | τ [μs] | C_{bulk} [$\mu\text{J/K}$] |
|-----------|--------------------------|---------------------------------------|
| 100 | 303.8 | 23.2 |
| 200 | 293.8 | 46.7 |
| 300 | 275.6 | 42.1 |
| 400 | 459.3 | 56.0 |
| 500 | 354.0 | 39.6 |

Equilibration times for pulse-to-pulse heating lie in the range $\tau = 370 \pm 90 \mu\text{s}$, as shown in table I, and this corresponds to a bulk heat capacity of $C_{\text{bulk}} = 41 \pm 18 \mu\text{J/K}$. This may be compared with that of the GaAs substrate (i.e., the largest mass in the device). A bulk Debye model gives a specific heat capacity of $c_p = 39 \text{ J}/(\text{kg K})$ at 30 K. If heat is stored evenly within the substrate volume, $0.2 \times 1 \times 0.85 = 0.17 \text{ mm}^3$ (with density, $5.32 \times 10^{-3} \text{ g mm}^{-3}$), this results in a heat capacity of $36 \mu\text{J/K}$, in good agreement with our measurement.

In conclusion, a superconducting NbN detector has been used to perform the first direct observation of pulse-to-pulse power degradation from a THz QCL. Power stabilization occurs on sub-millisecond timescales that cannot be resolved by conventional bolometric or pyroelectric detectors, with the power decay-rate being largest when high heat-sink temperatures or high pulse repetition rates are used. Although PL measurements allow analysis of rapid heat transfer processes at individual points within the QCL, our approach has allowed the first measurement of the bulk heat-storage effects that determine the total thermal equilibration time of the de-

vice. We have shown, using a lumped-component thermal model, that the inter-pulse heating occurs on a much longer time-scale than the intra-pulse thermal dynamics. The normalized thermal conductance obtained from our model lies within the range of values obtained using PL and time-averaged methods. The inferred heat capacity corresponds to that of the device substrate, confirming that this region forms a heat-transport bottleneck as expected from PL measurements.¹⁸ As such, this technique could be used as a reliable method for analyzing the thermal performance of device packaging or the power-stability of direct-modulation schemes for THz QCLs.

This project is funded by the Engineering and Physical Sciences Research Council, U.K., The European Research Council grants ‘TOSCA’ and ‘NOTES’, the Royal Society and the Wolfson Foundation, the German Federal Ministry of Education and Research (Grants 05K2010 and 13N12025) and by the DFG Center for Functional Nanostructures. We thank Mark Rosamond and Craig A. Evans (University of Leeds), Miriam S. Vitiello (Scuola Normale Superiore, Pisa, Italy) and Vincenzo Spagnolo (Politechnic University of Bari, Italy) for useful discussions.

- ¹R. Köhler, A. Tredicucci, F. Beltram, H. E. Beere, E. H. Linfield, A. G. Davies, D. A. Ritchie, R. C. Iotti, and F. Rossi, *Nature* **417**, 156159 (2002).
- ²B. Williams, S. Kumar, Q. Hu, and J. Reno, *Electron. Lett.* **42**, 8991 (2006).
- ³B. S. Williams, *Nat. Photonics* **1**, 517525 (2007).
- ⁴Y. Chassagneux, Q. Wang, S. Khanna, E. Strupiechonski, J. Coudevylle, E. Linfield, A. Davies, F. Capasso, M. Belkin, and R. Colombelli, *IEEE Trans. THz Sci. Technol.* **2**, 83 (2012).
- ⁵S. Fathololoumi, E. Dupont, C. Chan, Z. Wasilewski, S. Laframboise, D. Ban, A. Matyas, C. Jirauschek, Q. Hu, and H. C. Liu, *Opt. Express* **20**, 3866 (2012).
- ⁶B. Williams, S. Kumar, Q. Hu, and J. Reno, *Opt. Express* **13**, 3331 (2005).
- ⁷C. Evans, V. Jovanovic, D. Indjin, Z. Ikonc, and P. Harrison, *IEEE J. Quantum Electron.* **42**, 857 (2006).
- ⁸M. S. Vitiello, G. Scamarcio, and V. Spagnolo, *Appl. Phys. Lett.* **92**, 101116 (2008).
- ⁹H. Li, J. C. Cao, Y. J. Han, Z. Y. Tan, and X. G. Guo, *J. Phys. D: Appl. Phys.* **42**, 205102 (2009).
- ¹⁰K. S. Il'in, M. Lindgren, M. Currie, A. D. Semenov, G. N. Gol'tsman, R. Sobolewski, S. I. Cherednichenko, and E. M. Gershenzon, *Appl. Phys. Lett.* **76**, 2752 (2000).
- ¹¹A. D. Semenov, G. N. Gol'tsman, and R. Sobolewski, *Supercond. Sci. Technol.* **15**, R1 (2002).
- ¹²H. Luo, S. R. Laframboise, Z. R. Wasilewski, G. C. Aers, H. C. Liu, and J. C. Cao, *Appl. Phys. Lett.* **90**, 041112 (2007).
- ¹³A. Scheuring, P. Dean, A. Valavanis, A. Stockhausen, P. Thoma, M. Salih, S. P. Khanna, S. Chowdhury, J. D. Cooper, A. Grier, S. Wuensch, K. Il'in, E. H. Linfield, A. G. Davies, and M. Siegel, *IEEE Trans. THz Sci. Technol.* **3**, 172 (2013).
- ¹⁴A. D. Semenov, R. S. Nebosis, Y. P. Gousev, M. A. Heusinger, and K. F. Renk, *Phys. Rev. B* **52**, 581 (1995).
- ¹⁵R. Paiella, R. Martini, F. Capasso, C. Gmachl, H. Y. Hwang, D. L. Sivco, J. N. Baillargeon, A. Y. Cho, E. A. Whittaker, and H. C. Liu, *Appl. Phys. Lett.* **79**, 2526 (2001).
- ¹⁶M. Vitiello, G. Scamarcio, and V. Spagnolo, *IEEE J. Sel. Top. Quantum Electron.* **14**, 431 (2008).
- ¹⁷M. S. Vitiello, G. Scamarcio, V. Spagnolo, S. S. Dhillon, and C. Sirtori, *Appl. Phys. Lett.* **90**, 191115 (2007).
- ¹⁸M. S. Vitiello and G. Scamarcio, *Appl. Phys. Lett.* **96**, 101101 (2010).